Molecular Biology of the Cell
Vol. 20, 2639–2649, June 1, 2009

Identification of the Neuroblastoma-amplified Gene Product as a Component of the Syntaxin 18 Complex Implicated in Golgi-to-Endoplasmic Reticulum Retrograde Transport

Takehiro Aoki,*† Sarah Ichimura,*† Ayano Itoh,* Mami Kuramoto,* Takashi Shinkawa,‡ Toshiaki Isobe,‡ and Mitsuo Tagaya*

*School of Life Sciences, Tokyo University of Pharmacy and Life Sciences, Hachioji, Tokyo 192-0392, Japan; and ‡Department of Chemistry, Graduate School of Science, Tokyo Metropolitan University, Hachioji, Tokyo 192-0397, Japan

Submitted November 10, 2008; Revised March 26, 2009; Accepted April 2, 2009
Monitoring Editor: Vivek Malhotra

Syntaxin 18, a soluble *N*-ethylmaleimide-sensitive factor (NSF) attachment protein receptor (SNARE) protein implicated in endoplasmic reticulum (ER) membrane fusion, forms a complex with other SNAREs (BNIP1, p31, and Sec22b) and several peripheral membrane components (Sly1, ZW10, and RINT-1). In the present study, we showed that a peripheral membrane protein encoded by the neuroblastoma-amplified gene (*NAG*) is a subunit of the syntaxin 18 complex. *NAG* encodes a protein of 2371 amino acids, which exhibits weak similarity to yeast Dsl3p/Sec39p, an 82-kDa component of the complex containing the yeast syntaxin 18 orthologue Ufe1p. Under conditions favoring SNARE complex disassembly, NAG was released from syntaxin 18 but remained in a p31-ZW10-RINT-1 subcomplex. Binding studies showed that the extreme N-terminal region of p31 is responsible for the interaction with NAG and that the N- and the C-terminal regions of NAG interact with p31 and ZW10-RINT-1, respectively. Knockdown of NAG resulted in a reduction in the expression of p31, confirming their intimate relationship. NAG depletion did not substantially affect Golgi morphology and protein export from the ER, but it caused redistribution of Golgi recycling proteins accompanied by a defect in protein glycosylation. These results together suggest that NAG links between p31 and ZW10-RINT-1 and is involved in Golgi-to-ER transport.

INTRODUCTION

In the eukaryotic secretory pathway, newly synthesized proteins are exported from the endoplasmic reticulum (ER) and transported to the Golgi apparatus, in which they are sorted according to their destination (Palade, 1975). Protein transport is mediated by vesicles or membrane carriers that bud from the donor compartment and then tether to and fuse with the acceptor compartment (Bonifacino and Glick, 2004). Some of the vesicular components that have been delivered to the acceptor compartment concomitant with transport are recycled back to the donor compartment through the retrograde pathway. The anterograde and retrograde membrane flow is balanced, which ensures steady-state distribution of proteins and may allow the formation of new transport vesicles from the donor membrane (Sannerud *et al*., 2003).

Soluble *N*-ethylmaleimide-sensitive factor attachment protein (SNAP) receptors (SNAREs) play a pivotal role in membrane fusion of transport vesicles with the acceptor compartment (Jahn and Scheller, 2006). In mammalian cells, there are at least 36 SNARE members that are uniquely localized in different membrane compartments (Hong, 2005). Most SNAREs contain a single SNARE motif (a coiled-coil domain of 60–70 amino acids), which is followed by a C-terminal transmembrane domain (TMD) (Weimbs *et al*., 1997). Zippering of four SNARE motifs, one provided by vesicles and three by the target membrane (Sutton *et al*., 1998), seems to overcome the energy barrier and trigger membrane fusion (Weber *et al*., 1998; McNew *et al*., 2000). Depending on their function and localization on two opposing membranes, i.e., vesicles and target membranes, SNAREs can be classified into vesicle (v)-SNARE and target membrane (t)-SNARE, respectively (Söllner *et al*., 1993). Alternatively, SNAREs are categorized as R- and Q-SNAREs due to the presence of Arg and Gln, respectively, in the core binding domains of the four SNARE motifs (Fasshauer *et al*., 1998).

Syntaxins are members of the t/Q-SNARE family of proteins. Many of them have a three helical bundle in their N-terminal region, called the Habc domain (Dietrich *et al*.,

This article was published online ahead of print in *MBC in Press* (http://www.molbiolcell.org/cgi/doi/10.1091/mbc.E08–11–1104) on April 15, 2009.

† These authors contributed equally to this work.

Address correspondence to: Mitsuo Tagaya (tagaya@ls.toyaku.ac.jp).

Abbreviations used: ER, endoplasmic reticulum; ERGIC, ER-Golgi intermediate compartment; GFP, green fluorescent protein; KDEL-R, KDEL receptor; mAb, monoclonal antibody; Man II, mannosidase II; NAG, neuroblastoma-amplified gene; PNGase F, peptide:*N*-glycosidase F; siRNA; short interfering RNA; SNARE, *N*-ethylmaleimide-sensitive factor attachment protein receptor; TMD, transmembrane domain; VSVG, vesicular stomatitis virus-encoded glycoprotein; YFP, yellow fluorescent protein.

2003; Gerst, 2003). The Habc domain in several syntaxins can fold back to interact with the C-terminal SNARE motif, generating a closed conformation, whereas the Habc domain in others does not interact with the C-terminal region. Preceding the Habc domain, some syntaxin species have an extended N-terminal region that interacts with the Sec1/Munc18-like (SM) family of proteins, containing Sec1/Munc 18, Vps45, and Sly1. Although discrete modes of binding had been described for various SM–SNARE complexes (Toonen and Verhage, 2003), several recent findings revealed a common mode of binding for these complexes (for references, see Burkhardt *et al*., 2008). In addition to the regulation of conformation, SM proteins have been reported to contribute to the stability of syntaxins (Bryant and James, 2001; Toonen *et al*., 2005; Braun and Jentsch, 2007; Carpp *et al*., 2007).

We reported previously that syntaxin 18 is located in the ER and forms a large complex containing three other SNAREs (p31, BNIP1, and Sec22b) and three peripheral membrane proteins (Sly1, ZW10, and RINT-1) (Hatsuzawa *et al*., 2000; Hirose *et al*., 2004; Nakajima *et al*., 2004). Syntaxin 18 is the mammalian orthologue of yeast Ufe1p implicated in retrograde transport from the Golgi to the ER (Lewis and Pelham, 1996) and homotypic ER membrane fusion (Patel *et al*., 1998). The ER membrane fusion machinery seems to be conserved during evolution (Kraynack *et al*., 2005) because almost all equivalent components are present in the syntaxin 18 and Ufe1p complexes: p31, BNIP1, Sec22b, Sly1, ZW10, and RINT-1 in mammals correspond to Use1p/Slt1p, Sec20p, Sec22p, Sly1p, Dsl1p, and Tip20p in yeast, respectively (Sweet and Pelham, 1992, 1993; Lewis *et al*., 1997; Andag *et al*., 2001; Reilly *et al*., 2001; VanRheenen *et al*., 2001; Belgareh-Touze *et al*., 2003; Burri *et al*., 2003; Dilcher *et al*., 2003; Hirose *et al*., 2004; Nakajima *et al*., 2004). Our functional analyses suggested that ZW10 and RINT-1 are involved in membrane traffic between the ER and Golgi apparatus (Hirose *et al*., 2004; Arasaki *et al*., 2006, 2007; Inoue *et al*., 2008) and that BNIP1 participates in the formation of the three-way junctions of the ER network (Nakajima *et al*., 2004). Sun *et al*. (2007) demonstrated that ZW10 and RINT-1 play a role in a Rab6-dependent recycling pathway from the Golgi apparatus to the ER. Another group reported that syntaxin 18 and p31 participate in phagocytosis and post-Golgi transport, respectively (Hatsuzawa *et al*., 2006; Okumura *et al*., 2006). The versatile ability of the syntaxin 18 complex may be related to a unique mechanism of SNARE core complex assembly (Aoki *et al*., 2008).

One missing component of the mammalian ER fusion machinery is the equivalent of yeast Dsl3p/Sec39p, which has been reported to be required for the stability of t/Q-SNARE complex at the ER (Kraynack *et al*., 2005). In the present study, we demonstrated that a peripheral membrane protein encoded by the neuroblastoma-amplified gene (*NAG*) is a component of the syntaxin 18 complex. Despite a remarkable difference in molecular size, NAG (270 kDa) exhibits low sequence identity to Dsl3p/Sec39p (82 kDa). Our results showed that NAG serves as a link between p31 and ZW10-RINT-1 by interacting with the extreme N-terminal region of p31.

MATERIALS AND METHODS

Antibodies and Proteins

A polyclonal antibody against human NAG was raised against a bacterially expressed His-tagged NAG fragment (amino acids 2125-2371) and affinity purified using antigen-coupled beads. Rabbit polyclonal antibodies against vesicular stomatitis virus-encoded glycoprotein (VSVG) (amino acids 501-511), human Sly1 (amino acids 1-146 and 147-396), and human Rer1 (amino acids 1-14 and 183-196) were prepared and affinity purified. A monoclonal antibody (mAb) against VSVG (8G5) was prepared from ascites. mAbs against calnexin, GM130, GS15, GS27, GOS28, and Bet1 were obtained from BD Biosciences Transduction Laboratories (Lexington, KY). mAbs against α-tubulin and CD44 were purchased from Santa Cruz Biotechnology (Santa Cruz, CA). mAbs against protein disulfide isomerase, lysosome-associated membrane protein (LAMP)-2, mannosidase IB, and FLAG M2 were purchased from Daiichi Fine Chemical (Tokyo, Japan), Abcam (Cambridge, United Kingdom), Abnova (Taipei City, Taiwan), and Sigma-Aldrich (St. Louis, MO), respectively. A mAb against ER-Golgi intermediate compartment (ERGIC)-53 and a rabbit polyclonal antibody against KDEL receptor (KDEL-R) were generous gifts from Dr. Hans-Peter Hauri (University of Basel, Basel, Switzerland) and Dr. Hans-Dieter Söling (Max-Planck-Institute, Göttingen, Germany), respectively. Rabbit polyclonal antibodies against ERGIC-53 and FLAG were purchased from Sigma-Aldrich. Rabbit polyclonal antibodies against GPP130, Sec61β, and mannosidase II (Man II) were purchased from Covance Research Products (Berkeley, CA), Millipore (Billerica, MA), and Millipore Bioscience Research Reagents (Temecula, CA), respectively. Sheep antisera against TGN46 were purchased from AbD Serotec (Oxford, United Kingdom). Rabbit immunoglobulin G was purchased from Jackson ImmunoResearch Laboratories (West Grove, PA). Other antibodies were described previously (Hirose *et al*., 2004; Nakajima *et al*., 2004; Shimoi *et al*., 2005; Wakana *et al*., 2008).

Expression and purification of NSF and α-SNAP were described previously (Tani *et al*., 2003). Glutathione transferase (GST)-BNIP1ΔTMD (amino acids 1-202), GST-Sec22bΔTMD (amino acids 1-195), GST-p31ΔTMD (amino acids 1-231), and GST-p31ΔN15ΔTMD (amino acids 16-231) proteins were expressed in *Escherichia coli* and purified by glutathione-Sepharose 4B chromatography as described previously (Aoki *et al*., 2008).

Plasmids

pSPORT-NAG was purchased from RZPD (Deutsches Ressourcenzentrum fuer Genomforschung, Berlin, Germany). Because the clone was found to contain a frameshift and a nonsense mutation at nucleotides 1977 and 5941, respectively, the mutations were corrected as follows. The full-length NAG cDNA with mutations was amplified by polymerase chain reaction (PCR) from pSPORT-NAG and inserted into the BamH1/Sma1 site of pFLAG-CMV6 to produce pFLAG-NAG full**. The cDNA encoding amino acids 1-1035 of NAG was inserted into the Sma1 site of pFLAG-CMV6, and the point mutation at nucleotide 1977 was corrected by inverted PCR. The BamH1/Nde1 fragment of pFLAG-NAG full** was cut out and replaced with the corrected fragment to obtain pFLAG-NAG full*. Next, the cDNA encoding amino acids 1036-2371 of NAG was inserted into the EcoRV site of pFLAG-CMV6, and the point mutation at nucleotide 5941 was corrected. The Nhe1/Nhe1 fragment of pFLAG-NAG full* was replaced with the corresponding fragment of correct sequence to obtain pFLAG-NAG full. To express an NAG fragment in *E. coli*, the cDNA encoding amino acids 2125-2371 of NAG was amplified by PCR and inserted into the BamH1/Sma1 site of pET11d-His. The cDNAs encoding amino acids 6-259, 11-259, 16-259, and 20-259 of p31 were amplified from the cDNA of full-length p31 and inserted into the BglII/EcoRV site of pFLAG-CMV6. Other constructs were reported previously (Aoki *et al*., 2008). The plasmids encoding *N*-acetylglucosaminyltransferase I-green fluorescent protein (GFP) and β-1,4-galactosyltransferase 1-GFP were kindly supplied by Dr. Nobuhiro Nakamura (Kanazawa University, Kanazawa, Japan) and Dr. Jennifer Lippincott-Schwartz (National Institutes of Health, Bethesda, MD), respectively.

Cell Culture

293T cells were cultured in DMEM supplemented with 50 IU/ml penicillin, 50 μg/ml streptomycin, and 10% fetal calf serum. HeLa cells were cultured in Eagle's minimum essential medium supplemented with 50 IU/ml penicillin, 50 μg/ml streptomycin, 100 mg/ml L-glutamine, and 10% fetal calf serum.

RNA Interference

The following short interfering RNAs (siRNAs) were used: Lamin A/C, ctggacttccagaagaaca; NAG (4160), ctagtaaagcagtacaaga; NAG (4382), ctacagccaatgaagatct; ZW10, aagggtgaggtgtgcaatatg; RINT-1, ttagccactgatattccttgt; p31, accggcctctgaggtgatcaa; and GS15, aagcatgaccagcctgctta. siRNAs were purchased from Japan BioService (Asaka, Japan). HeLa cells were grown on 35-mm or 10-cm dishes, and siRNAs were transfected at a final concentration of 200 nM using Oligofectamine (Invitrogen, Carlsbad, CA) according to the manufacturer's protocol.

Preparation of Cell Lysates and Binding Assay

293T cells at ~70% confluence were transfected with 2 μg of pFLAG-NAG full or 1 μg for other constructs per 35-mm dish by using Lipofectamine Plus reagent (Invitrogen) according to the manufacturer's protocol. After 24 h of incubation, the cells were lysed with lysis buffer (20 mM HEPES-KOH, 150 mM KCl, 1% Triton X-100, 1 mM dithiothreitol, 2 mM EDTA, 10 μg/ml

leupeptin, 2 μM pepstatin A, 2 μg/ml aprotinin, and 1 mM phenylmethylsulfonyl fluoride, pH 7.2).

GST-tagged proteins (5 μg) were mixed with glutathione-Sepharose 4B in binding buffer (50 mM Na_2HPO_4, 100 mM NaCl, 0.1% Triton X-100, 1 mM EDTA, and 2 mM 2-mercaptethanol, pH 7.0) and then incubated overnight at 4°C with 200 μg of cell lysates. After extensive washing of the beads, the proteins bound to the beads were solubilized in sample buffer and subjected to SDS-polyacrylamide gel electrophoresis (PAGE).

Immunofluorescence Analysis

Immunofluorescence microscopy was performed as described previously (Tagaya *et al*., 1996). Cells were fixed with methanol at −20°C for 5 min for staining Man II, ZW10, RINT-1, and Rer1 or with 4% paraformaldehyde at room temperature for 20 min for other proteins.

Subcellular Fractionation

Tet-on HeLa cells (2 10-cm dishes) were washed twice with phosphate-buffered saline, collected, and suspended in homogenization buffer (10 mM Tris-HCl, 4 mM $MgCl_2$, 120 mM NaCl, and 5 mM KCl, pH 7.2) and then homogenized with 10 strokes with a 25-gauge needle. The homogenate was centrifuged at 3000 rpm for 10 min, and then the supernatant was centrifuged again at 3000 rpm for 10 min. The postnuclear supernatant was load onto a 17.5–44% of Nycoprep gradient and centrifuged in a Beckman SW50 rotor at 80,000 × *g* for 3 h. After centrifugation, fractions were collected from the top, and every other fraction was subjected to SDS-PAGE after trichloroacetic acid precipitation.

Protein Transport Assay

The expression plasmid for VSVG fused with GFP was kindly donated by Dr. J. Lippincott-Schwartz (National Institutes of Health). Morphological and biochemical transport assays were performed as described previously (Iinuma *et al*., 2007). VSVG-GFP transported to the plasma membrane was detected using anti-VSVG (8G5) without cell permeabilization.

Retrograde Transport Assay

The plasmid encoding ts045VSVG-KDEL-R-yellow fluorescent protein (YFP) was kindly donated by Dr. Alberto Luini (Consorzio Mario Negri Sud, Santa Maria Imbaro, Italy). HeLa cells grown on 35-mm dishes were mock transfected or transfected with NAG (4160) and incubated at 37°C for 48 h. The cells were then transfected with 1 μg of the plasmid encoding VSVG-KDEL-R-YFP and incubated at 32°C for 24 h. Cycloheximide was added to the medium at a final concentration of 20 μg/ml, and the cells were incubated for another 2 h. To monitor retrograde transport, the temperature was shifted to 40°C. After 2 h, the cells were fixed and processed for immunofluorescence analysis.

Digitonin Permeabilization

HeLa cells were washed twice with permeabilization buffer (20 mM HEPES-KOH, 50 mM NaCl, 2 mM $MgCl_2$, 250 mM sucrose, and 1 mM dithiothreitol, pH 7.4) and then incubated with 50 μg/ml digitonin (Merck, Darmstadt, Germany) at 4°C for 20 min. The cells were washed with permeabilization buffer twice and processed for immunofluorescence microscopy.

Peptide:N-glycosidase F (PNGase F) Treatment

HeLa cells depleted of NAG were solubilized with phosphate-buffered saline with 0.5% SDS and heated at 100°C for 10 min. A portion of lysates (8.2 μg) was diluted twice in reaction buffer (200 mM Tris-HCl, 2% Nonidet P-40, and 20 mM 2-mercaptoethanol, pH 8.6) and treated with PNGase F (Takara Bio, Otsu, Japan) at a final concentration of 12.5 μU/μl at 37°C for 24 h. After the reaction, the samples were subjected to SDS-PAGE.

In-Gel Digestion and Mass Spectrometry

Proteins coprecipitated with anti-p31 antibody-bound protein G-Sepharose were subjected to SDS-PAGE and visualized by silver staining. The stained bands were excised from the gel, in-gel digested with trypsin, and subjected to the direct nanoflow liquid chromatography-tandem mass spectrometry (LC-MS/MS) system (Natsume *et al*., 2002; Kaji *et al*., 2006). The peptide mixture was separated on a frit-less Mightysil-C18 (3-μm particle; Kanto Chemical, Tokyo, Japan) column (30 mm × 0.150 μm i.d.) by using a 80-min gradient of acetonitrile (0–40%) in 0.1% formic acid at a flow rate of 50 nl/min, and the eluted peptides were sprayed directly into a high resolution quadrapole time-of-flight hybrid mass spectrometer Q-TOF Ultima (Waters, Milford, MA). MS/MS spectra were acquired by data-dependent collision-induced dissociation, and the MS/MS data were analyzed using MASCOT software (Matrix Science, London, United Kingdom) for peptide assignment. The resulting data set was finally evaluated by in-house software STEM (Shinkawa *et al*., 2005).

RESULTS

Identification of the NAG Protein as a New Component of the Syntaxin 18 Complex

The SNARE complex is disassembled by NSF-α-SNAP in a manner coupled with NSF-mediated ATP hydrolysis (Söllner *et al*., 1993). We demonstrated previously that p31, ZW10, and RINT-1 remain associated after SNARE complex disassembly (Hirose *et al*., 2004). Our two-hybrid analysis showed that ZW10 and RINT-1 interact directly, but neither of them binds to p31, suggesting the presence of protein(s) that mediates the interaction of p31 with ZW10 and/or RINT-1.

To test this possibility, we raised mAbs against p31 and conducted an immunoprecipitation experiment using mAb 5C3 attached to protein G-Sepharose. Unexpectedly, SDS-PAGE analysis showed that many proteins were coprecipitated with the antibody-bound beads (Figure 1A, right lane). To remove nonspecific binding proteins, cell lysates were premixed with protein G-Sepharose, and then the supernatant was subjected to immunopurification. However, still many proteins were found to bind to the antibody-bound beads (data not shown). Therefore, we decided to determine p31-binding candidates and then carefully examine the specificity of binding. The proteins coprecipitated with the antibody-bound beads were separated by SDS-PAGE, digested in gels, and subjected to LC-MS/MS analysis. In addition to several proteins that are known to interact with p31 and syntaxin 18, such as RINT-1, ZW10, NSF, and Sly1, a protein of ~270 kDa encoded by *NAG* was identified (Supplemental Table S1).

To verify whether NAG is really associated with p31, we raised a polyclonal antibody against NAG. The NAG antibody recognized an ~270-kDa band (Supplemental Figure S1A, lane 1), in good agreement with the calculated molecular mass of NAG. The expression of the 270-kDa protein was knocked down by siRNA [NAG (4160)] (lane 2), confirming that the recognized protein is NAG. The staining intensities of a 90-kDa and a doublet of ~50-kDa bands were not reduced by NAG (4160), suggesting that they are proteins nonspecifically recognized by the antibody.

As shown in Figure 1B, lanes 2 and 5, NAG was coprecipitated with mAbs against p31 and syntaxin 18. Sec22b, a v/R-SNARE mainly localizes to the ER-Golgi intermediate compartment (ERGIC) (Hay *et al*., 1998; Zhang *et al*., 1999), was coprecipitated with syntaxin 18 (lane 5) but not with p31 (lane 2). This may reflect that syntaxin 18, but not p31, is the principal partner for Sec22b on the ER membrane (Aoki *et al*., 2008). Of note is that NAG remained associated with p31 under conditions favoring SNARE complex disassembly (lane 3), albeit its release from syntaxin 18 (lane 6). The association of NAG with p31 and syntaxin 18 was confirmed by an immunoprecipitation experiment using the NAG antibody (Supplemental Figure S1B, lane 2). These results unequivocally demonstrated that NAG is a component of the syntaxin 18 complex and forms a subcomplex with p31, ZW10, and RINT-1.

To determine the subcellular localization of NAG, cell homogenates were separated by density gradient centrifugation and analyzed by immunoblotting. As shown in Figure 1C, NAG cosedimented with p31 and an ER marker protein calnexin. To confirm the ER localization of NAG by immunofluorescence microscopy, we tried to obtain a specific anti-NAG antibody useful for immunostaining. As antigens, we tested several synthetic peptides or fragments expressed in *E. coli* but could not succeed to obtain good antibodies. We therefore expressed FLAG-tagged NAG in

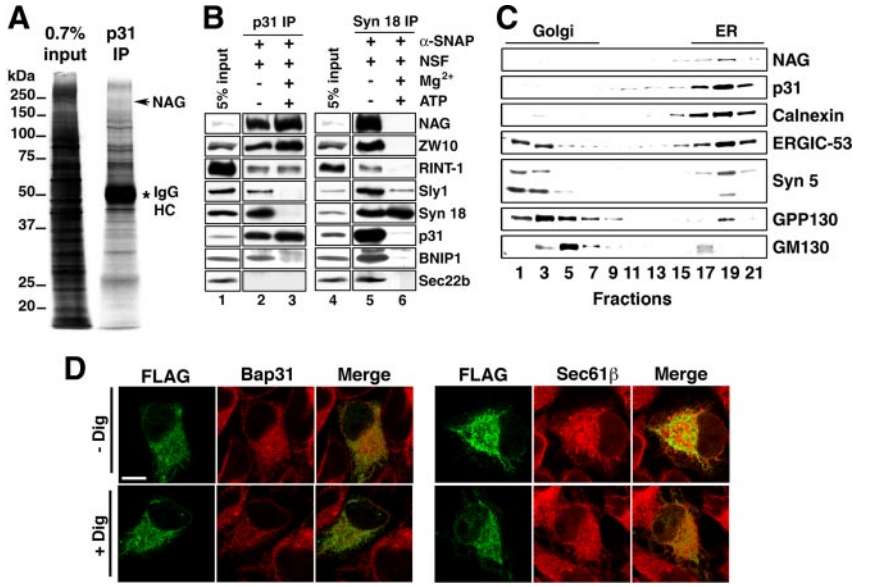

Figure 1. Identification of the NAG protein as a component of the syntaxin 18 complex. (A) Triton X-100 extracts of 293T cells were immunoprecipitated with an anti-p31 antibody (mAb 5C3) attached to protein G-Sepharose 4B. The coprecipitated proteins were resolved by SDS-PAGE, stained with silver, and analyzed by LC-MS/MS. An asterisk denotes immunoglobulin heavy chain. (B) Triton X-100 extracts of 293T cells were incubated at 16°C for 60 min with 10 μg/ml NSF and 5 μg/ml α-SNAP in the presence or absence of 8 mM Mg^{2+} and 0.5 mM ATP. After incubation, the samples were immunoprecipitated with a mAb against p31 (lanes 2 and 3) or syntaxin 18 (lanes 5 and 6). The precipitated proteins were separated by SDS-PAGE and analyzed by immunoblotting with the indicated antibodies. (C) Cell homogenates were subjected to Nycoprep density gradient centrifugation and analyzed by immunoblotting with the indicated antibodies. (D) HeLa cells were transfected with the plasmid encoding FLAG-NAG. At 24 h after transfection, the cells were left untreated (top row; − Dig) or treated with digitonin (bottom row; + Dig), and double-stained with antibodies against FLAG and Bap31 (left) or Sec61β (right). Bar, 20 μm.

HeLa cells and examined its distribution using an anti-FLAG antibody. Although FLAG-NAG was expressed in only a few percent of the transfected cells, the expressed protein was colocalized with ER marker proteins Bap31 and Sec61β (Figure 1D). The FLAG-NAG immunostaining was not diminished by digitonin permeabilization of cells, suggesting the membrane association of the expressed protein.

The N-Terminal Region of p31 Is Required for the Interaction with NAG

In addition to the SNARE motif at the C terminus, p31 has a putative coiled-coil region at the N terminus (amino acids 3–26, predicted by the Lupus algorithm with a window size of 21 residues). Given that the N-terminal region of SNAREs is responsible for the interaction with SNARE regulators (Dietrich *et al.*, 2003; Gerst, 2003), N-terminally truncated versions of p31 were expressed as FLAG-tag proteins in 293T cells, immunoprecipitated with an anti-FLAG antibody, and analyzed by immunoblotting. As shown in Figure 2A, NAG as well as ZW10 and RINT-1 was coprecipitated with full-length p31 and p31ΔN5 to the same extent (lanes 5 and 6), whereas no precipitation was observed with p31ΔN10 and p31ΔN15 (lanes 7 and 8). In contrast, the binding of individual mutants to syntaxin 18 was not markedly different. These results suggest that the extreme N-terminal region of p31 is required for the interaction with NAG and other accessory proteins.

To confirm this finding, we next performed pull-down experiments using recombinant p31 and ER SNAREs. Isolated recombinant GST fusion proteins with SNAREs lacking the TMD were mixed with cell lysates, pulled down with glutathione beads, and analyzed by immunoblotting (Figure 2B). Consistent with the results of the immunoprecipitation experiments, NAG and RINT-1 were pulled down with GST-p31ΔTMD (lane 4) but not with GSTp31ΔN15ΔTMD (lane 5). Essentially no binding to NAG or RINT-1 was detected for GST-BNIP1ΔTMD (lane 2) and GST-Sec22bΔTMD (lane 3). Nevertheless, GST-BNIP1ΔTMD bound syntaxin 18 to an extent comparable to that observed for GST-p31ΔTMD. These results support the idea that p31, but not BNIP1 or syntaxin 18, binds directly NAG and accessory proteins.

NAG Serves as a Link between p31 and ZW10-RINT-1

To determine which regions of NAG are responsible for the interaction with p31 and ZW10-RINT-1, NAG was divided into two fragments. As a shown in Figure 2C, lane 5, the N-terminal fragment of NAG (NAG N; 1–1035 amino acids) bound p31 and, to a much lesser extent, syntaxin 18, but not ZW10 or RINT-1. Conversely, the C-terminal fragment of NAG (NAG C; 1036–2371 amino acids) was associated with ZW10 and RINT-1 but not with p31 or syntaxin 18 (lane 6). These results raised the possibility that NAG serves as a link between p31 and ZW10-RINT-1 through its distinct regions.

To verify this hypothesis, we conducted GST-p31ΔTMD pull-down experiments using cell lysates depleted of NAG. As expected, neither ZW10 nor RINT-1 was pulled down with GST-p31ΔTMD when NAG expression was knocked down by NAG (4160) (Figure 2D, lane 6). By contrast, depletion of ZW10 or RINT-1 did not affect the binding between GST-p31ΔTMD and NAG (lanes 7 and 8). These results support the idea that NAG serves as a link between p31 and ZW10-RINT-1. Of note, ZW10 was associated with GST-p31ΔTMD even when RINT-1 was depleted. This may suggest that ZW10 is a major binding partner for NAG.

NAG Depletion Induces the Release of ZW10-RINT-1 from Membranes

To further demonstrate that NAG acts as a linker between p31 and ZW10-RINT-1, NAG expression was knocked down by NAG (4160), and cell lysates were immunoprecipitated with an antibody against syntaxin 18 (Figure 3A, lane 4) or p31 (lane 6). Clearly, the amounts of ZW10-RINT-1 coprecipitated with both antibodies were much lower than those in mock-transfected cells (lanes 3 and 5). Next, we examined whether this dissociation of ZW10-RINT-1 from p31 leads to their release from ER membranes. To this end, homogenates of NAG-depleted cells were prepared without detergent and separated into the membrane and cytosol fractions by centrifugation. As shown in Figure 3B, concomitant with NAG

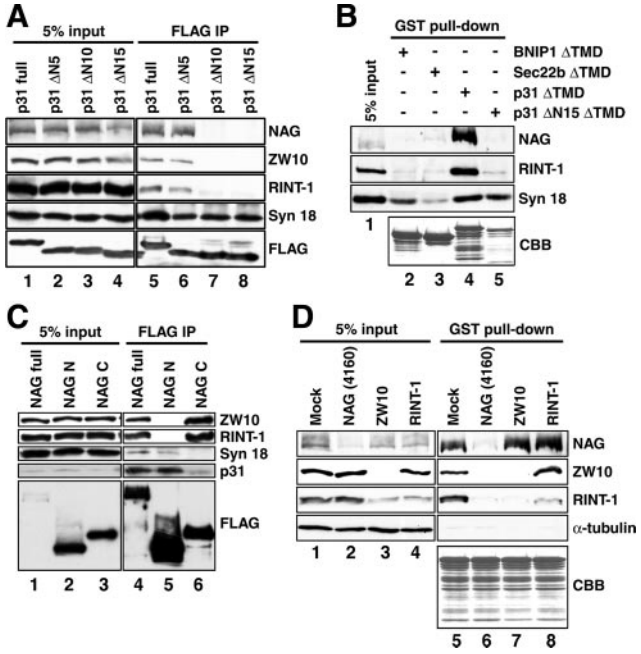

Figure 2. NAG links between p31 and ZW10-RINT-1 through an extreme N-terminal region of p31. (A) 293T cells were transfected with the plasmids encoding full-length or N-terminally truncated versions of FLAG-p31. At 24 h after transfection, the cells were lysed, and immunoprecipitation experiments were carried out using an anti-FLAG antibody. The precipitated proteins were separated by SDS-PAGE and analyzed by immunoblotting with the indicated antibodies. (B) Recombinant GST-BNIP1ΔTMD, GST-Sec22bΔTMD, GST-p31ΔTMD, and GST-p31ΔN15ΔTMD immobilized onto glutathione-Sepharose 4B were incubated with lysates of 293T cells at 4°C overnight. Pull-down experiments were conducted, and the proteins bound to the resin were separated by SDS-PAGE and visualized by immunoblotting or Coomassie Brilliant Blue (CBB) staining. (C) Lysates of 293T cells transfected with the plasmids encoding full-length or truncated versions of FLAG-NAG were immunoprecipitated using an anti-FLAG antibody. The precipitated proteins were separated by SDS-PAGE and analyzed by immunoblotting with the indicated antibodies. (D) Recombinant GST-p31ΔTMD immobilized onto glutathione-Sepharose 4B was incubated at 4°C overnight with lysates of HeLa cells depleted of NAG, ZW10, or RINT-1. Pull-down experiments were conducted, and the proteins bound to the resin were separated by SDS-PAGE and visualized by immunoblotting or CBB staining.

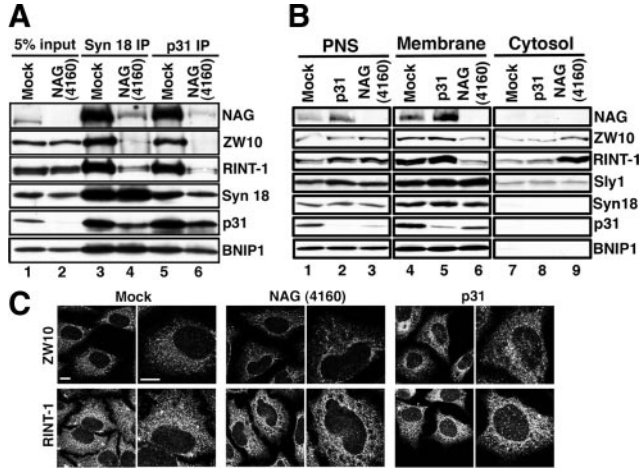

Figure 3. Knockdown of NAG causes the release of ZW10-RINT-1 from membranes as well as from p31. HeLa cells were mock-transfected or transfected with NAG (4160) or p31 siRNA. (A) At 72 h after transfection, cell lysates were prepared and immunoprecipitated with an antibody against syntaxin 18 (lanes 3 and 4) or p31 (lanes 5 and 6). The precipitated proteins were separated by SDS-PAGE and analyzed by immunoblotting with the indicated antibodies. (B) At 72 h after transfection, the cells were homogenized by passage 40 times through a 27-gauge needle. The homogenate was centrifuged at 1100 × *g* for 5 min to obtain the postnuclear supernatant (PNS; lanes 1–3) and then at 135,000 × *g* for 30 min to separate the membrane (lanes 4–6) and cytosol (lanes 7–9). (C) At 72 h after transfection, the cells were stained with the indicated antibodies. Note that many and some RINT-1-negative large puncta were observed in NAG- and p31-depleted cells, respectively (bottom row). Bars, 10 μm.

depletion, the amounts of membrane-bound ZW10-RINT-1 were decreased (lane 6 vs. lane 4), and accordingly, their cytosolic contents were increased (lane 9 vs. lane 7). Consistent with the idea that Sly is not a component of the NAG subcomplex (Hirose *et al*., 2004), no release of Sly1 from membranes was observed in NAG-depleted cells. It should be noted that NAG was almost exclusively membrane-associated and not released from membranes after p31 depletion (lanes 5 and 8). This may suggest that NAG binds to ER proteins other than p31. Alternatively, because NAG is a large protein with several hydrophobic regions (Scott *et al*., 2003), it may bind to ER membranes through its hydrophobic regions.

We demonstrated previously that depletion of RINT-1 causes redistribution of ZW10 (Arasaki *et al*., 2006). If NAG really supports the binding of ZW10-RINT-1 to ER membranes, knockdown of NAG may cause a similar change in the distribution of ZW10. This was indeed the case (Figure 3C, top row). Depletion of NAG changed ZW10 staining from the uniform staining of the ER to a dispersed, dot-like staining (top row, middle two panels), as observed in the case of RINT-1 depletion (Arasaki *et al*., 2006). Such a change was not observed in the RINT-1 staining, although RINT-1-negative large puncta were observed (bottom row). These puncta correspond to patchy accumulation of ER luminal proteins, such as protein disulfide isomerase and Hsp47 (data not shown). Similar puncta were observed in cells depleted of syntaxin 18 (Iinuma *et al*., 2009) or p31 (Uemura *et al*., 2009; Figure 3C, bottom row, right two panels).

Knockdown of NAG Induces a Reduction in the Expression of p31

In the course of NAG knockdown experiments, we noticed that knockdown of NAG by NAG (4160) resulted in a reduction in the expression level of p31 (Figure 4A, lane 2). Another siRNAs [NAG (4382)] also induced a significant reduction in p31 expression (lane 3). The extent of p31 reduction seemed to correlate with NAG knockdown efficiency. By contrast, the expression levels of other components of the syntaxin 18 complex (Figure 4A) or Golgi-localized SNAREs (Figure 4B) were not significantly affected by knockdown of NAG. These results suggest that NAG plays a role in stabilizing p31 and confirm an intimate relationship between the two proteins.

Depletion of NAG Changes the Distribution of Recycling Proteins without Substantially Affecting Golgi Morphology

To reveal the role of NAG in the early secretory pathway, we first examined the distribution of proteins in the Golgi and the ER-Golgi interface in cells transfected with NAG (4160). As shown in Figure 5A, no substantial change in the distri-

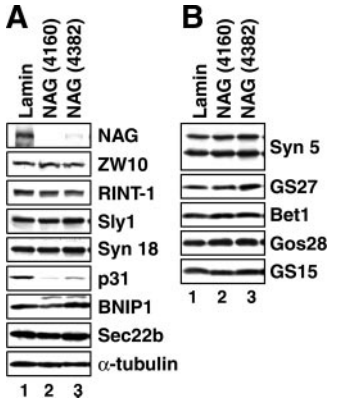

Figure 4. Depletion of NAG induces a reduction in the expression level of p31. HeLa cells were transfected with lamin A/C siRNA, NAG (4160), or NAG (4382). At 72 h after transfection, the cells were solubilized in phosphate-buffered saline with 0.5% SDS, and the lysates (15 μg each) were separated by SDS-PAGE and analyzed by immunoblotting with the indicated antibodies.

bution of *cis*-, *medial*-, and *trans*-Golgi resident proteins (GM130, Man II, and TGN46, respectively) and an ER exit site marker, Sec31A, was detected at 72 h after siRNA transfection. Strikingly, knockdown of NAG caused dispersion of *cis*-Golgi-localized recycling proteins, KDEL-R and Rer1, and an ER-Golgi intermediate compartment marker, ERGIC-53 (Appenzeller-Herzog and Hauri, 2006) (Figure 5B, middle column). A similar phenotype was observed when NAG was knocked down with NAG (4382) (Supplemental Figure S2). The phenotype of cells transfected with NAG siRNA was more severe compared with that of cells transfected with siRNA targeting p31 (Figure 5B, middle column vs. right one), implying the contribution of NAG depletion to these changes. The p31 siRNA used could fully suppress the expression of p31 (Figure 3B, lane 2).

Blockage of the Tethering of Retrograde Carriers from the Golgi Apparatus in NAG-depleted Cells

To assess the state of *cis*-Golgi and ERGIC-localized recycling proteins in NAG-depleted cells, we permeabilized cells

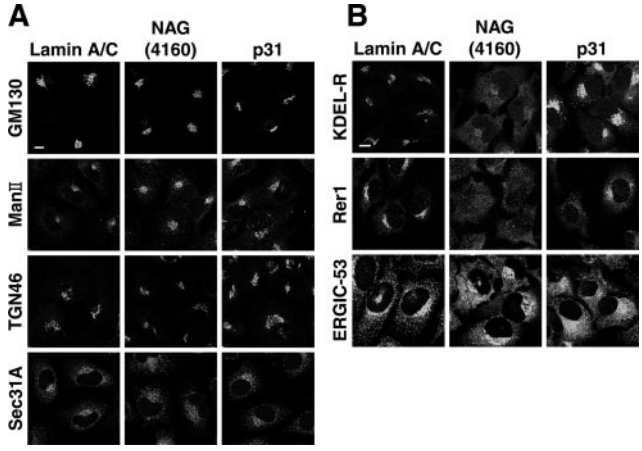

Figure 5. Depletion of NAG changes the distribution of recycling proteins without affecting the Golgi apparatus. HeLa cells were transfected with lamin A/C siRNA, NAG (4160), or p31 siRNA. At 72 h after transfection, the cells were fixed and immunostained with antibodies against proteins in the Golgi or ER exit sites (A) or recycling proteins (B). Bars, 10 μm.

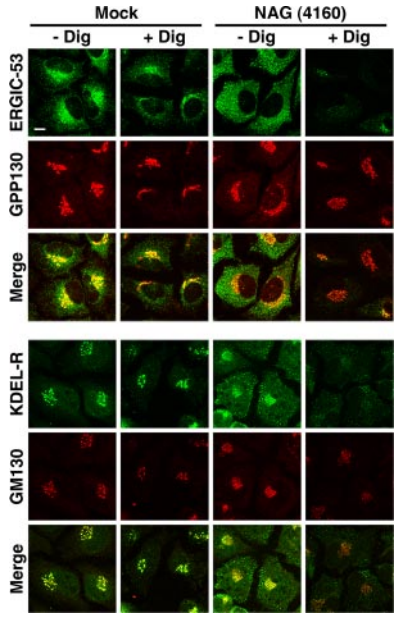

Figure 6. Digitonin sensitivity of recycling proteins in NAG-depleted cells. HeLa cells were mock transfected (left two columns) or transfected with NAG (4160) (right two columns). At 72 h after transfection, the cells were permeabilized with digitonin and double-stained with antibodies against ERGIC-53 (top row) and GPP130 (second row) or KDEL-R (fourth row) and GM130 (fifth row). Bar, 10 μm.

with digitonin. Digitonin at low concentrations is known to solubilize the plasma membrane but not other membranes including ER and Golgi membranes. Zolov and Lupashin (2005) demonstrated that nontethered Golgi vesicles in COG3-depleted cells are efficiently released from digitonin-permeabilized cells. As shown in Figure 6, the immunostaining intensity of ERGIC-53 (top row) and KDEL-R (fourth row) in NAG-depleted cells (right two columns), but not in mock-transfected cells (left two columns), was markedly reduced upon permeabilization, suggesting that ERGIC-53– and KDEL-R–containing membranes are not tightly associated with cellular structures after NAG depletion. In contrast, decreases in the immunostaining intensity of Golgi proteins, such as GPP130 (second row) and GM130 (fifth row), were not markedly different between mock-transfected and NAG-depleted cells. These results suggest that NAG depletion likely blocks the tethering step in retrograde transport from the Golgi apparatus to the ER.

To verify that retrograde transport to the ER is inhibited after NAG knockdown, we carried out a retrograde transport assay by using ts045 VSVG-KDEL-R chimera. At 32°C (permissive temperature), this chimera is localized in the *cis*-Golgi but redistributes to the ER through the retrograde pathway upon shift to 40°C (nonpermissive temperature) (Cole *et al.*, 1998; Yang *et al.*, 2005, 2008). When expressed at the permissive temperature, VSVG-KDEL-R-YFP was localized in the perinuclear region in many NAG-depleted cells as well as mock-transfected cells (Figure 7, type I). In some cells, however, VSVG-KDEL-R-YFP was localized in the ER with some in punctate structures (type II) or distributed as punctate structures throughout the cytoplasm (type III). When the temperature was shifted to 40°C, VSVG-KDEL-R-YFP redistributed to the ER (type II) in most mock-transfected cells, whereas redistribution of VSVG-KDEL-R-YFP to the ER was substantially inhibited in NAG-depleted cells

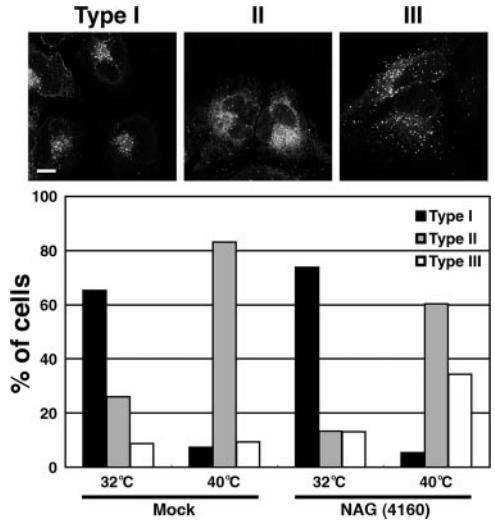

Figure 7. Retrograde transport of VSVG-KDEL-R is impaired in NAG-depleted cells. The experiments were conducted as described in *Materials and Methods*. Expressed VSVG-KDEL-R-YFP was predominantly in the perinuclear region (type I), in the ER (type II), or in diffuse distribution (type III). Bottom, quantitative data. The average of three independent experiments is shown. For each sample, >200 cells were evaluated. Bar, 10 μm.

(Figure 7, bottom). These results suggest that the retrograde transport of VSVG-KDEL-R-YFP to the ER is inhibited by NAG depletion.

Depletion of NAG Causes a Defect in the Glycosylation of Secretory and Lysosomal Proteins

Because Golgi morphology was not markedly disrupted in cells treated with NAG siRNA for 72 h, we examined whether protein transport from the ER to the Golgi is unaffected in NAG-depleted cells. To this end, NAG (4160) and the plasmid encoding VSVG-GFP were sequentially transfected into HeLa cells, and the cells were incubated at the nonpermissive temperature to allow the accumulation of VSVG-GFP at the ER. The transport of VSVG-GFP was monitored by immunofluorescence microscopy after the cells were shifted to the permissive temperature. As shown in Figure 8A, left, no significant retardation of VSVG-GFP transport was observed in NAG-depleted cells, whereas a marked delay was detected in GS15-depleted cells (a positive control). However, when Endo H resistance of VSVG-GFP was analyzed, a large fraction of VSVG-GFP remained Endo H sensitive (Figure 8A, right). A similar result was obtained when NAG (4382) was used to suppress NAG expression. These results suggest that the processing of glycosylation is defective in NAG-depleted cells. To confirm this, we examined the glycosylation of endogenous secretory and lysosomal glycoproteins in NAG-depleted cells. As shown in Figure 8B, left, the gel mobility of both CD44, a plasma membrane-localized protein, and LAMP-2, a lysosomal resident, on SDS-PAGE was increased after 72 h of NAG knockdown, implying the production of underglycosylated protein species. The mobility shifts of the two proteins were more enhanced after a prolonged incubation (7 d). To verify that the increased gel mobility of CD44 was due to defective glycosylation, lysates of NAG-depleted HeLa cells were subjected to PNGase F treatment to remove N-linked oligosaccharides. The molecular weight of the deglycosylated form of CD44 in NAG-depleted cells was found to be almost

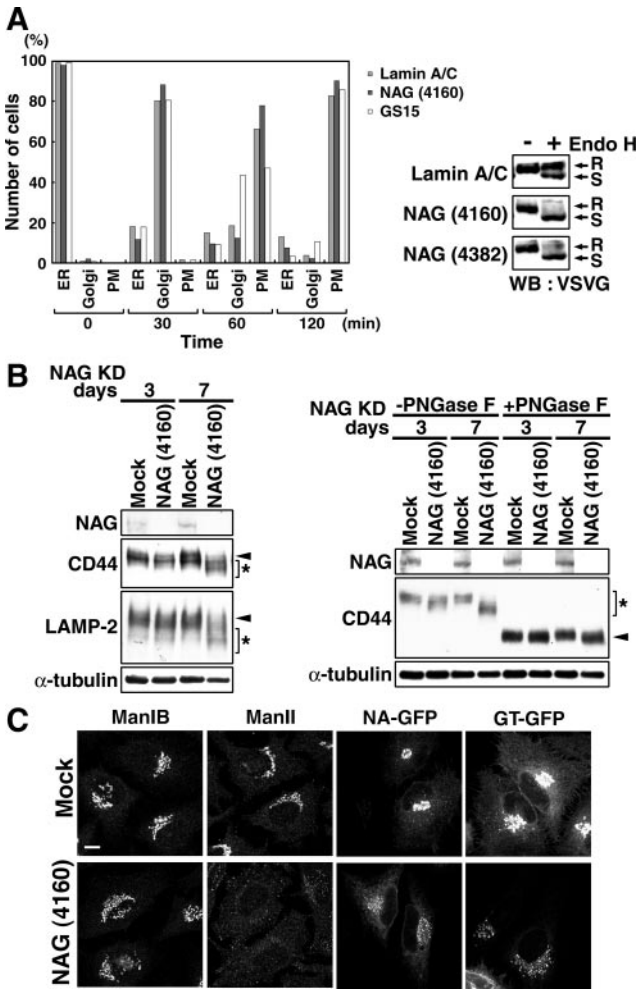

Figure 8. Depletion of NAG causes a defect in glycosylation of secretory and lysosomal proteins. (A) HeLa cells were successively transfected with lamin A/C siRNA, NAG (4160), or GS15 siRNA and then with the plasmid for VSVG-GFP. Transport of VSVG-GFP was monitored as described in *Materials and Methods*. The number of cells in which VSVG-GFP was localized in the ER, the Golgi apparatus, and plasma membrane (PM) were counted. Alternatively, lysates of cells double transfected were prepared after 120-min incubation at the permissive temperature and treated with endoglycosidase H (Endo H). The samples were subjected to SDS-PAGE and analyzed by immunoblotting with an anti-VSVG antibody. R, Endo H-resistant bands; S, Endo H-sensitive bands. (B, left) HeLa cells were mock treated or treated with NAG (4160) for 3 or 7 d, solubilized in phosphate-buffered saline with 0.5% SDS, separated by SDS-PAGE, and analyzed by immunoblotting with the indicated antibodies. Arrowheads and asterisks indicate fully glycosylated and underglycosylated proteins, respectively. (B, right) Lysates of HeLa cells depleted of NAG for 3 or 7 d were treated with PNGase F. Samples were loaded on SDS-PAGE and analyzed by immunoblotting with the indicated antibodies. Asterisk and arrowheads indicate the positions of glycosylated and deglycosylated forms of CD44, respectively. (C) Distribution of glycosylation enzymes in HeLa cells treated with NAG (4160) for 7 d. In the expression of *N*-acetylglucosaminyltransferase I-GFP (NA-GFP) and β-1,4-galactosyltransferase 1-GFP (GT-GFP), the plasmids encoding GFP fusion proteins were transfected into HeLa cells at 6 d after transfection with NAG (4160). Bar, 10 μm.

identical with that in mock transfected cells (Figure 8B, right), indicating that the increased gel mobility of CD44 after NAG knockdown is mainly due to glycosylation defect.

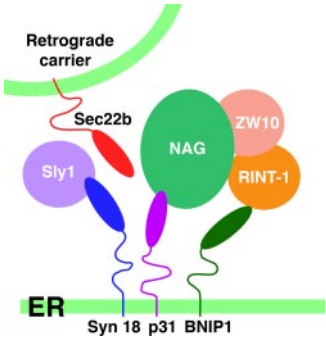

Figure 9. Schematic representation of the syntaxin 18 complex. NAG associates with p31 and ZW10-RINT-1 through its N-terminal and C-terminal regions, respectively. RINT-1 may weakly interact with BNIP1.

Because glycosylation defect was enhanced after a prolong NAG knockdown, we examined the distribution of Golgi glycosylation enzymes at 7 d after transfection of cells with NAG siRNA. In contrast to the phenotype observed at 3-d knockdown of NAG, glycosylation enzymes were detected in centrally, disconnected elements (mannosidase IB, *N*-acetylglucosaminyltransferase I-GFP, and β-1,4-galactosyltransferase 1-GFP) or in puncta distributed throughout the cytoplasm (Man II) (Figure 8C).

DISUCUSSION

The *NAG* gene was first identified as a gene coamplified with the *MYCN* gene in neuroblastoma (Wimmer *et al.*, 1999). The function of NAG is not known, and there is some controversy concerning whether NAG is associated with tumor progression and prognosis (Scott *et al.*, 2003; Weber *et al.*, 2004; Kaneko *et al.*, 2007). Here, we show that NAG is a subunit of the syntaxin 18 complex and serves as a link between p31 and ZW10-RINT-1 (Figure 9). The N-terminal region (amino acids 1-1035) and C-terminal region (amino acids 1036-2371) of NAG bind p31 and ZW10-RINT-1, respectively. The latter region corresponds to that encoded by a 4.5-kb transcript, which was originally assumed to code for the entire protein (Wimmer *et al.*, 1999). However, a later study demonstrated that a 7.3-kb mRNA encoding 2371 amino acids is the major transcript (Scott *et al.*, 2003). Our immunoblotting analysis showed the presence of the major ~270-kDa protein, but not the ~150-kDa protein encoded by the 4.5-kb transcript, suggesting that the 4.5-kb product is not efficiently translated. We confirmed that the major NAG species in IMR-32, a neuroblastoma cell line where *NAG* was coamplified with *MYCN* (Scott *et al.*, 2003), is also an ~270-kDa protein (data not shown). The finding that NAG is encoded by the 7.5-kb transcript makes sense because the N-terminal region that is absent in the product of the 4.5-kb transcript is required for the important function of NAG, i.e., the interaction with p31.

Sequence comparison revealed that the central region of NAG (amino acids 577-1707) shares 17% amino acid identity with yeast 82-kDa Dsl3p/Sec39p (Mnaimneh *et al.*, 2004; Kraynack *et al.*, 2005). NAG seems to be the orthologue of yeast Dsl3p/Sec39p, although their molecular sizes are remarkably different. The finding that the C-terminal region of NAG (amino acids 1036-2371) binds ZW10-RINT-1 is in line with the observation of Kraynack *et al.* (2005) that the C-terminal region of Dsl3p/Sec39p (amino acids 548-675) interacts with Dsl1p, the yeast ZW10 orthologue (Andag and Schmitt, 2003; Hirose *et al.*, 2004), in a yeast two-hybrid assay. In yeast, Dsl3p/Sec39p as well as Dsl1p greatly facilitates the recruitment of Use1p/Slt1p (yeast p31) to the ternary complex consisting of the Ufe1p (syntaxin 18), Sec20p (BNIP1), and Tip20p (RINT-1), whereas Tip20p plays a central role within the complex (Kraynack *et al.*, 2005). In mammalian cells, NAG is a critical factor to link between p31 and accessory proteins but does not seem to be important for SNARE core complex assembly for the following reasons. First, BNIP1 was fully associated with syntaxin 18 in the absence of NAG (Figure 3A). Second, p31 lacking the N-terminal NAG-binding region (p31ΔN15ΔTMD), as well as full-length p31, was found to bind syntaxin 18 (Figure 2, A and B).

A knockdown experiment demonstrated that NAG contributes to stabilize p31. A similar down-regulation was reported for Use1p/Slt1p in a yeast *dsl3* mutant (*dsl3-1*) (Kraynack *et al.*, 2005). Several syntaxin family members are known to be stabilized by SM proteins (Bryant and James, 2001; Toonen *et al.*, 2005; Braun and Jentsch, 2007; Carpp *et al.*, 2007). Braun and Jentsch (2007) recently demonstrated that Ufe1p is ubiquitinated and degraded by an ERAD-like mechanism in the absence of an SM protein, Sly1p. Our preliminary data also showed that p31 can be ubiquitinated (unpublished data). Further studies will clarify the mechanism of p31 down-regulation and its implication in the formation of the syntaxin 18 complex.

ERGIC-53, KDEL-R, and Rer1 are known to cycle between either the ERGIC or Golgi and the ER in a COPI-dependent, Rab6-independent manner (Sato *et al.*, 1995, 2001; Füllekrug *et al.*, 1997; Kappeler *et al.*, 1997; Orci *et al.*, 1997; Tisdale *et al.*, 1997; Majoul *et al.*, 2001; del Nery *et al.*, 2006). In cells treated with NAG (4160) for 72 h, these proteins showed a diffuse distribution, whereas Golgi-resident proteins, which can be transported to the ER in a Rab6-dependent manner (Girod *et al.*, 1999; White *et al.*, 1999; Malsam *et al.*, 2005; Young *et al.*, 2005), remained in a ribbon-like structure (Figure 5), suggesting that NAG is involved in the COPI-dependent pathway. Indeed, Golgi-to-ER retrograde transport of KDEL-R, a protein that uses a COPI route (Girod *et al.*, 1999), was impaired in NAG-depleted cells. The diffuse distribution of ERGIC and Golgi recycling proteins in NAG-depleted cells may represent nontethered vesicles or tubules. In support of this idea, these vesicles or tubules were found to be easily released from digitonin-permeabilized cells. In contrast, ERGIC-53 and Golgi recycling protein were not released from digitonin-permeabilized control cells. Although Okumura *et al.* (2006) reported no change in the localization of KDEL-R upon p31 depletion, our results showed redistribution of recycling proteins, including KDEL-R upon knockdown of p31. The difference between their result and ours may be in part due to the fact that the distribution of KDEL-R was analyzed at 24 h after transfection of siRNA by Okumura *et al.* (2006), but 72 h in our case. Alternatively, the difference may be derived from the use of different cell lines; NIH3T3 cells by Okumura *et al.* (2006) and HeLa cells by us. It is also possible that Okumura *et al.* (2006) might not notice a distributional change of KDEL-R in p31-depleted cells because the change was probably more subtle compared with the phenotype of NAG-depleted cells, as shown in this study.

Despite the intimate relationship between NAG and ZW10, the relatively intact Golgi phenotype in NAG-depleted cells is significantly different from that in cells where ZW10 is knocked down (Hirose *et al.*, 2004; Varma *et al.*, 2006; Sun *et al.*, 2007). There are several possible explanations. The first is that the two proteins may control different Golgi-to-ER retrograde trafficking pathways by interacting

with other unidentified proteins. Although our data unequivocally demonstrated that NAG and ZW10 are components of the syntaxin 18 complex, it is possible that they interact with other sets of proteins in the ER. Some fractions of ZW10-RINT1 remained associated with membranes in the absence of NAG (Figure 3B). Another possibility is that ZW10 plays a role not only in Golgi-to-ER retrograde transport but also in ER-to-Golgi anterograde transport, as proposed previously (Hirose *et al*., 2004), whereas NAG is exclusive for the retrograde pathway. ZW10 is a dynamitin-interacting protein and helps the recruitment of the microtubule minus-end–directed motor dynein-dynactin to kinetochores (Starr *et al*., 1998) and perhaps to other cellular structures, including the ER and Golgi. Dynein-dynactin is known to mediate ER-to-Golgi anterograde transport (Burkhardt *et al*., 1997, Presley *et al*., 1997). In certain cells, ZW10 is localized not only in the ER but also in the Golgi apparatus (Varma *et al*., 2006; Arasaki *et al*., 2007), near where the minus-end of microtubules is located. Golgi localization of ZW10 may be a result of its movement to the minus-end of microtubules accompanied by anterograde transport.

NAG depletion did not significantly inhibit anterograde transport of VSVG-GFP from the ER to the plasma membrane through the Golgi apparatus, but it affected glycosylation of VSVG-GFP and endogenous proteins. A prolonged depletion of NAG caused a severe glycosylation defect. Shestakova *et al*. (2006) reported that Golgi modification of CD44 and LAMP-2 is defective in a prolonged (6–9 d) knockdown of COG3, a subunit of the conserved oligomeric Golgi (COG) complex most likely implicated in retrograde transport within the Golgi apparatus (Ungar *et al*., 2006; Smith and Lupashin, 2008). Glycosylation defect in COG3-depleted cells is likely due to the relocation of Golgi enzymes to COG complex-dependent vesicles (Shestakova *et al*., 2006), which likely mediate retrograde transport within the Golgi apparatus under normal conditions (Zolov and Lupashin, 2005). Although the distribution of Golgi enzymes was not markedly altered in cells treated with NAG siRNA for 72 h (Figure 5; data not shown), a prolonged knockdown induced their redistribution (Figure 8C). One simple explanation for impaired glycosylation of VSVG-GFP in cells treated with NAG siRNA for 72 h is that glycosylation enzymes could not fully gain access to VSVG-GFP, although they remained in a ribbon-like structure at the level of immunofluorescence microscopy. Because a large amount of VSVG-GFP passed through the Golgi apparatus in a short time, a small change in the distribution of glycosylation enzymes may largely affect glycosylation efficiency of secretory proteins. Alternatively, recycling of oligosaccharide processing enzymes in the ER–Golgi interface may be impaired. It has been reported that yeast α-mannosidase I interacts with Rer1 (Massaad and Herscovics, 2001). In mammals, UDP-glucose:glycoprotein glucosyltransferase, a protein folding sensor and glucosyltransferase, is enriched in the ER-Golgi interface, in addition to the presence in the ER (Zuber *et al*., 2001). It is possible that perturbation of retrograde transport of proteins, such as Rer1 and KDEL-R, responsible for recycling of oligosaccharide processing enzymes causes a defect in glycosylation.

In future studies, it is important to examine whether NAG plays a role in determining tumor behavior, and if so, what is the mechanism? It should be noted that NAG partners, ZW10 and RINT-1, are spindle and G2/M checkpoint proteins, respectively (Williams *et al*., 1992; Chan *et al*., 2000; Xiao *et al*., 2001). ZW10 in a complex with ROD and Zwilch plays a role in turning off of the spindle checkpoint (Williams *et al*., 2003). It has been reported that ~81% of the RINT-1 heterozygotes succumb to multiple tumor formation with haploinsufficiency during their average life span of 24 mo (Lin *et al*., 2007). Moreover, together with the p130 member of the Rb family, RINT-1 is known to control telomere length in a telomerase-independent manner (Kong *et al*., 2006). It is tempting to speculate that overexpression of NAG perturbs the quantitative balance of complexes involved in cell cycle-related events and membrane traffic, leading to uncontrolled cell proliferation. Alternatively, overexpression of NAG may affect the attachment of cells to matrix by perturbing cell–matrix binding molecules. It has been reported that *MYCN* amplification down-regulates CD44 or may affect the glycosylation of CD44 (Gross *et al*., 1997, 2000). CD44 is involved in cell–cell and cell–matrix interactions and its glycosylation regulates the binding to hyaluronan (Skelton *et al*., 1998).

In conclusion, our results disclose that the product of a gene coamplified with *MYCN* is a subunit of the ER SNARE complex and participates in Golgi-to-ER retrograde membrane traffic.

ACKNOWLEDGMENTS

We thank Drs. M. G. Waters, H.-P. Hauri, J. Lippincott-Schwartz, H. D. Söling, N. Nakamura, A. Luini, and B. Mayer for gifts of reagents. We are grateful to K. Suzuki, Y. Aikawa, H. Inaba, K. Miyazaki, and R. Kato for technical assistance. This work was supported in part by Grants-in-Aid for Scientific Research 18370081, 18050036, 18657044, and 19036032 from the Ministry of Education, Science, Sports and Culture of Japan.

REFERENCES

Andag, U., Neumann, T., and Schmitt, H. D. (2001). The coatomer-interacting protein Dsl1p is required for Golgi-to-endoplasmic reticulum retrieval in yeast. J. Biol. Chem. *276*, 39150–39160.

Andag, U., and Schmitt, H. D. (2003). Dsl1p, an essential component of the Golgi-endoplasmic reticulum retrieval system in yeast, uses the same sequence motif to interact with different subunits of the COPI vesicle coat. J. Biol. Chem. *278*, 51722–51734.

Aoki, T., Kojima, M., Tani, K., and Tagaya, M. (2008). Sec22b-dependent assembly of endoplasmic reticulum Q-SNARE proteins. Biochem. J. *410*, 93–100.

Appenzeller-Herzog, C., and Hauri, H. P. (2006). The ER-Golgi intermediate compartment (ERGIC): in search of its identity and function. J. Cell Sci. *119*, 2173–2183.

Arasaki, K., Taniguchi, M., Tani, K., and Tagaya, M. (2006). RINT-1 regulates the localization and entry of ZW10 to the syntaxin 18 complex. Mol. Biol. Cell *17*, 2780–2788.

Arasaki, K., Uemura, T., Tani, K., and Tagaya, M. (2007). Correlation of Golgi localization of ZW10 and centrosomal accumulation of dynactin. Biochem. Biophys. Res. Commun. *359*, 811–816.

Belgareh-Touze, N., Corral-Debrinski, M., Launhardt, H., Galan, J. M., Munder, T., Le Panse, S., and Haguenauer-Tsapis, R. (2003). Yeast functional analysis: identification of two essential genes involved in ER to Golgi trafficking. Traffic *4*, 607–617.

Bonifacino, J. S., and Glick, B. S. (2004). The mechanism of vesicle budding and fusion. Cell *116*, 153–166.

Braun, S., and Jentsch, S. (2007). SM-protein-controlled ER-associated degradation discriminates between different SNAREs. EMBO Rep. *8*, 1176–1182.

Bryant, N. J., and James, D. E. (2001). Vps45p stabilizes the syntaxin homologue Tlg2p and positively regulates SNARE complex formation. EMBO J. *20*, 3380–3388.

Burkhardt, J. K., Echeverri, C. J., Nilsson, T., and Vallee, R. B. (1997). Overexpression of the dynamitin (p50) subunit of the dynactin complex disrupts dynein-dependent maintenance of membrane organelle distribution. J. Cell Biol. *139*, 469–484.

Burkhardt, P., Hattendorf, D. A., Weis, W. I., and Fasshauer, D. (2008). Munc18a controls SNARE assembly through its interaction with the syntaxin N-peptide. EMBO J. *27*, 923–933.

Burri, L., Varlamov, O., Doege, C. A., Hofmann, K., Beilharz, T., Rothman, J. E., Söllner, T. H., and Lithgow, T. (2003). A SNARE required for retrograde transport to the endoplasmic reticulum. Proc. Natl. Acad. Sci. USA *100*, 9873–9877.

Carpp, L. N., Shanks, S. G., Struthers, M. S., and Bryant, N. J. (2007). Cellular levels of the syntaxin Tlg2p are regulated by a single mode of binding to Vps45p. Biochem. Biophys. Res. Commun. *363*, 857–860.

Chan, G.K.T., Jablonski, S. A., Starr, D. A., Goldberg, M. L., and Yen, T. J. (2000). Human Zw10 and ROD are mitotic checkpoint proteins that bind to kinetochores. Nat. Cell Biol. *2*, 944–947.

Cole, N. B., Ellenberg, J., Song, J., DiEuliis, D., and Lippincott-Schwartz, J. (1998). Retrograde transport of Golgi-localized proteins to the ER. J. Cell Biol. *140*, 1–15.

del Nery, E., Miserey-Lenkei, S., Falguières, T., Nizak, C., Johannes, L., Perez, F., and Goud, B. (2006). Rab6A and Rab6A′ GTPases play non-overlapping roles in membrane trafficking. Traffic *7*, 394–407.

Dietrich, L. E., Boeddinghaus, C., LaGrassa, T. J., and Ungermann, C. (2003). Control of eukaryotic membrane fusion by N-terminal domains of SNARE proteins. Biochim. Biophys. Acta *1641*, 111–119.

Dilcher, M., Veith, B., Chidambaram, S., Hartmann, E., Schmitt, H. D., and Fischer von Mollard, G. (2003). Use1p is a yeast SNARE protein required for retrograde traffic to the ER. EMBO J. *22*, 3664–3674.

Fasshauer, D., Sutton, R. B., Brunger, A. T., and Jahn, R. (1998). Conserved structural features of the synaptic fusion complex: SNARE proteins reclassified as Q- and R-SNAREs. Proc. Natl. Acad. Sci. USA *95*, 15781–15786.

Füllekrug, J., Boehm, J., Röttger, S., Nilsson, T., Mieskes, G., and Schmitt. H. D. (1997). Human Rer1 is localized to the Golgi apparatus and complements the deletion of the homologous Rer1 protein of *Saccharomyces cerevisiae*. Eur. J. Cell Biol. *74*, 31–40.

Gerst, J. E. (2003). SNARE regulators: matchmakers and matchbreakers. Biochem. Biophys. Acta *1641*, 99–110.

Girod, A., Storrie, B., Simpson, J. C., Johannes, L., Goud, B., Roberts, L. M., Lord, J. M., Nilsson, T., and Pepperkok, R. (1999). Evidence for a COP-I-independent transport route from the Golgi complex to the endoplasmic reticulum. Nat. Cell Biol. *1*, 423–430.

Gross, N., Balmas, K., and Brognara, C. B. (1997). Absence of functional CD44 hyaluronan receptor on human NMYC-amplified neuroblastoma cells. Cancer Res. *57*, 1387–1393.

Gross, N., Balmas–Bourloud, K., and Brognara, C. B. (2000). MYCN-related suppression of functional CD44 expression enhances tumorigenic properties of human neuroblastoma cells. Exp. Cell Res. *260*, 396–403.

Hatsuzawa, K., Hirose, H., Tani, K., Yamamoto, A., Scheller, R. H., and Tagaya, M. (2000). Syntaxin 18, a SNAP receptor that functions in the endoplasmic reticulum, intermediate compartment, and cis-Golgi vesicle trafficking. J. Biol. Chem. *275*, 13713–13720.

Hatsuzawa, K., Tamura, T., Hashimoto, H., Hashimoto, H., Yokoya, S., Miura, M., Nagaya, H., and Wada, I. (2006). Involvement of syntaxin 18, an endoplasmic reticulum (ER)-localized SNARE protein, in ER-mediated phagocytosis. Mol. Biol. Cell *17*, 3964–3977.

Hay, J. C., Klumperman, J., Oorschot, V., Steegmaier, M., Kuo, C. S., and Scheller, R. H. (1998). Localization, dynamics, and protein interactions reveal distinct roles for ER and Golgi SNAREs. J. Cell Biol. *141*, 1489–1502.

Hirose, H., Arasaki, K., Dohmae, N., Takio, K., Hatsuzawa, K., Nagahama, M., Tani, K., Yamamoto, A., Tohyama, M., and Tagaya, M. (2004). Implication of ZW10 in membrane trafficking between the endoplasmic reticulum and Golgi. EMBO J. *23*, 1267–1278.

Hong, W. (2005). SNAREs and traffic. Biochim. Biophys. Acta *1744*, 120–144.

Iinuma, T., Shiga, A., Nakamoto, K., O'brien, M. B., Aridor, M., Arimitsu, N., Tagaya, M., and Tani, K. (2007). Mammalian Sec16/p250 plays a role in membrane traffic from the endoplasmic reticulum. J. Biol. Chem. *282*, 17632–17639.

Iinuma, T., Aoki, T., Arasaki, K., Hirose, H., Yamamoto, A., Samata, R., Hauri, H. P., Arimitsu, N., Tagaya, M., and Tani, K. (2009). Role of syntaxin 18 in the organization of endoplasmic reticulum subdomains. J. Cell Sci. *122*, 1680–1690.

Inoue, M., Arasaki, K., Ueda, A., Aoki, T., and Tagaya, M. (2008). N-terminal region of ZW10 serves not only as a determinant for localization but also as a link with dynein function. Genes Cells *13*, 905–914.

Jahn, R., and Scheller, R. H. (2006). SNAREs—engines for membrane fusion. Nat. Rev. Mol. Cell Biol. *7*, 631–643.

Kaji, H., Yamauchi, Y., Takahashi, N., and Isobe, T. (2006). Mass spectrometric identification of N-linked glycopeptides using lectin-mediated affinity capture and glycosylation site-specific stable isotope tagging. Nat. Protoc. *1*, 3019–3302.

Kaneko, S., Ohira, M., Nakamura, Y., Isogai, E., Nakagawara, A., and Kaneko, M. (2007). Relationship of DDX1 and NAG gene amplification/overexpression to the prognosis of patients with MYCN-amplified neuroblastoma. J. Cancer Res. Clin. Oncol. *133*, 185–192.

Kappeler, F., Klopfenstein, D. R., Foguet, M., Paccaud, J.-P., and Hauri, H. P. (1997). The recycling of ERGIC-53 in the early secretory pathway. ERGIC-53 carries a cytosolic endoplasmic reticulum-exit determinant interacting with COP II. J. Biol. Chem. *272*, 31801–31808.

Kong, L. J., Meloni, A. R., and Nevins, J. R. (2006). The Rb-related p130 protein controls telomere lengthening through an interaction with a Rad50-interacting protein, RINT-1. Mol. Cell *22*, 63–71.

Kraynack, B. A., Chan, A., Rosenthal, E., Essid, M., Umansky, B., Waters, M. G., and Schmitt, H. D. (2005). Dsl1p, Tip20p, and the novel Dsl3 (Sec39) protein are required for the stability of the Q/t-SNARE complex at the endoplasmic reticulum in yeast. Mol. Biol. Cell *16*, 3963–3977.

Lewis, M., and Pelham, H.R.B. (1996). SNARE-mediated retrograde traffic from the Golgi complex to the endoplasmic reticulum. Cell *85*, 205–215.

Lewis, M. J., Rayner, J. C., and Pelham, H. R. (1997). A novel SNARE complex implicated in vesicle fusion with the endoplasmic reticulum. EMBO J. *16*, 3017–3024.

Lin, X., Liu, C. C., Gao, Q., Zhang, X., Wu, G., and Lee, W. H. (2007). RINT-1 serves as a tumor suppressor and maintains Golgi dynamics and centrosome integrity for cell survival. Mol. Cell. Biol. *27*, 4905–4916.

Malsam, J., Satoh, A., Pelletier, L., and Warren, G. (2005). Golgin tethers define subpopulations of COPI vesicles. Science *307*, 1095–1098.

Majoul, I., Straub, M., Hell, S. W., Duden, R., and Söling, H. D. (2001). KDEL-cargo regulates interactions between proteins involved in COPI vesicle traffic: measurements in living cells using FRET. Dev. Cell *1*, 139–153.

Massaad, M. J., and Herscovics, A. (2001). Interaction of the endoplasmic reticulum α-1,2-mannosidase Mns1p with Rer1p using the split-ubiquitin system. J. Cell Sci. *114*, 4629–4635.

McNew, J. A., Parlati, F., Fukuda, R., Johnston, R. J., Paz, K., Paumet, F., Söllner, T. H., and Rothman. J. E. (2000). Compartmental specificity of cellular membrane fusion encoded in SNARE proteins. Nature *407*, 153–159.

Mnaimneh, S., *et al*. (2004). Exploration of essential gene functions via titratable promoter alleles. Cell *118*, 31–34.

Nakajima, K., Hirose, H., Taniguchi, M., Kurashina, H., Arasaki, K., Nagahama, M., Tani, K., Yamamoto, A., and Tagaya, M. (2004). Involvement of BNIP1 in apoptosis and endoplasmic reticulum membrane fusion. EMBO J. *23*, 3216–3226.

Natsume, T., Yamauchi, Y., Nakayama, H., Shinkawa, T., Yanagida, M., Takahashi, N., and Isobe, T. (2002). A direct nanoflow liquid chromatography-tandem mass spectrometry system for interaction proteomics. Anal. Chem. *74*, 4725–4733.

Okumura, A. J., Hatsuzawa, K., Tamura, T., Nagaya, H., Saeki, K., Okumura, F., Nagao, K., Nishikawa, M., Yoshimura, A., and Wada, I. (2006). Involvement of a novel Q-SNARE, D12, in quality control of the endomembrane system. J. Biol. Chem. *281*, 4495–4506.

Orci, L., Stamnes, M,. Ravazzola, M., Amherdt, M., Perrelet, A, Söllner, T. H., and Rothman, J. E. (1997). Bidirectional transport by distinct populations of COPI-coated vesicles. Cell *90*, 335–349.

Palade, G. (1975). Intracellular aspects of the process of protein synthesis. Science *189*, 347–358.

Patel, S. K., Indig, F. E., Olivieri, N., Levine, N. D., and Latterich, M. (1998). Organelle membrane fusion: a novel function for the syntaxin homolog Ufe1p in ER membrane fusion. Cell *92*, 611–620.

Presley, J. F., Cole, N. B., Schroer, T. A., Hirschberg, K., Zaal, K. J., and Lippincott-Schwartz, J. (1997). ER-to-Golgi transport visualized in living cells. Nature *389*, 81–85.

Reilly, B. A., Kraynack, B. A., VanRheenen, S. M., and Waters, M. G. (2001). Golgi-to-endoplasmic reticulum (ER) retrograde traffic in yeast requires Dsl1p, a component of the ER target site that interacts with a COPI coat subunit. Mol. Biol. Cell *12*, 3783–3796.

Sannerud, R., Saraste, J., and Goud, B. (2003). Retrograde traffic in the biosynthetic-secretory route: pathways and machinery. Curr. Opin. Cell Biol. *15*, 438–445.

Sato, K., Nishikawa, S., and Nakano, A. (1995). Membrane protein retrieval from the Golgi apparatus to the endoplasmic reticulum (ER): characterization of the RER1 gene product as a component involved in ER localization of Sec12p. Mol. Biol. Cell *6*, 1459–1477.

Sato, K., Sato, M., and Nakano, A. (2001). Rer1p, a retrieval receptor for endoplasmic reticulum membrane proteins, is dynamically localized to the Golgi apparatus by coatomer. J. Cell Biol. *152*, 935–944.

Scott, D. K., Board, J. R., Lu, X., Pearson, A. D., Kenyon, R. M., and Lunec, J. (2003). The neuroblastoma amplified gene, NAG: genomic structure and characterisation of the 7.3 kb transcript predominantly expressed in neuroblastoma. Gene *307*, 1–11.

Shestakova, A., Zolov, S., and Lupashin, V. (2006). COG complex-mediated recycling of Golgi glycosyltransferases is essential for normal protein glycosylation. Traffic *7*, 191–204.

Shimoi, W., Ezawa, I., Nakamoto, K., Uesaki, S., Gabreski, G., Aridor, M., Yamamoto, A., Nagahama, M., Tagaya, M., and Tani, K. (2005). p125 is localized in endoplasmic reticulum exit sites and involved in their organization. J. Biol. Chem. *280*, 10141–10148.

Shinkawa, T., Taoka, M., Yamauchi, Y., Ichimura, T., Kaji, H., Takahashi, N., and Isobe, T. (2005). STEM: a software tool for large-scale proteomic data analyses. J. Proteome Res. *4*, 1826–1831.

Skelton, T. P., Zeng, C., Nocks, A., and Stamenkovic, I. (1998). Glycosylation provides both stimulatory and inhibitory effects on cell surface and soluble CD44 binding to hyaluronan. J. Cell Biol. *140*, 431–446.

Smith, R. D., and Lupashin, V. V. (2008). Role of the conserved oligomeric Golgi (COG) complex in protein glycosylation. Carbohydr. Res. *343*, 2024–2031.

Söllner, T., Whiteheart, S. W., Brunner, M., Erdjument-Bromage, H., Geromanos, S., Tempst, P., and Rothman, J. E. (1993). SNAP receptors implicated in vesicle targeting and fusion. Nature *362*, 318–324.

Starr, D. A., Williams, B. C., Hays, T. S., and Goldberg, M. L. (1998). ZW10 helps recruit dynactin and dynein to the kinetochore. J. Cell Biol. *142*, 763–774.

Sun, Y., Shestakova, A., Hunt, L., Sehgal, S., Lupashin, V., and Storrie, B. (2007). Rab6 regulates both ZW10/RINT-1- and conserved oligomeric Golgi complex-dependent Golgi trafficking and homeostasis. Mol. Biol. Cell *18*, 4129–4142.

Sutton, R. B., Fasshauer, D., Jahn, R., and Brunger, A. T. (1998). Crystal structure of a SNARE complex involved in synaptic exocytosis at 2.4 Å resolution. Nature *395*, 347–353.

Sweet, D. J., and Pelham, H. R. (1992). The *Saccharomyces cerevisiae* SEC20 gene encodes a membrane glycoprotein which is sorted by the HDEL retrieval system. EMBO J. *11*, 423–432.

Sweet, D. J., and Pelham, H. R. (1993). The TIP1 gene of *Saccharomyces cerevisiae* encodes an 80 kDa cytoplasmic protein that interacts with the cytoplasmic domain of Sec20p. EMBO J. *12*, 2831–2840.

Tagaya, M., Furuno, A., and Mizushima, S. (1996). SNAP prevents Mg^{2+}-ATP-induced release of N-ethylmaleimide-sensitive factor from the Golgi apparatus in digitonin-permeabilized PC12 cells. J. Biol. Chem. *271*, 466–470.

Tani, K., Shibata, M., Kawase, K., Kawashima, H., Hatsuzawa, K., Nagahama, M., and Tagaya, M. (2003). Mapping of functional domains of γ-SNAP. J. Biol. Chem. *278*, 13531–13538.

Tisdale, E. J., Plutner, H., Matteson, J., and Balch, W. E. (1997). p53/58 binds COPI and is required for selective transport through the early secretory pathway. J. Cell Biol. *137*, 581–593.

Toonen, R. F., and Verhage, M. (2003). Vesicle trafficking: pleasure and pain from SM genes. Trends Cell Biol. *13*, 177–186.

Toonen, R. F., de Vries, K. J., Zalm, R., Südhof, T. C., and Verhage, M. (2005). Munc18-1 stabilizes syntaxin 1, but is not essential for syntaxin 1 targeting and SNARE complex formation. J. Neurochem. *93*, 1393–1400.

Uemura, T., Sato, T., Aoki, T., Yamamoto, A., Okada, T., Hirai, R., Harada, R., Mori, K., Tagaya, M., and Harada, A. (2009). p31 deficiency influences endoplasmic reticulum tubular morphology and cell survival. Mol. Cell. Biol. *29*, 1869–1881.

Ungar, D., Oka, T., Krieger, M., and Hughson, F. M. (2006). Retrograde transport on the COG railway. Trends Cell Biol. *16*, 113–120.

Varma, D., Dujardin, D. L., Stehman, S. A., and Vallee, R. B. (2006). Role of the kinetochore/cell cycle checkpoint protein ZW10 in interphase cytoplasmic dynein function. J. Cell Biol. *172*, 655–662.

VanRheenen, S. M., Reilly, B. A., Chamberlain, S. J., and Waters, M. G. (2001). Dsl1p, an essential protein required for membrane traffic at the endoplasmic reticulum/Golgi interface in yeast. Traffic *2*, 212–231.

Wakana, Y., Takai, S., Nakajima, K., Tani, K., Yamamoto, A., Watson, P., Stephens, D. J., Hauri, H. P., and Tagaya, M. (2008). Bap31 is an itinerant protein that moves between the peripheral endoplasmic reticulum (ER) and a juxtanuclear compartment related to ER-associated degradation. Mol. Biol. Cell *19*, 1825–1836.

Weber, T., Zemelman, B. V., McNew, J. A., Westermann, B., Gmachl, M., Parlati, F., Söllner, T. H., and Rothman, J. E. (1998). SNAREpins: minimal machinery for membrane fusion. Cell *92*, 759–772.

Weber, A., Imisch, P., Bergmann, E., and Christiansen, H. (2004). Coamplification of DDX1 correlates with an improved survival probability in children with MYCN-amplified human neuroblastoma. J. Clin. Oncol. *22*, 2681–2690.

Weimbs, T., Low, S. H., Chapin, S. J., Mostov, K. E., Bucher, P., and Hofmann, K. (1997). A conserved domain is present in different families of vesicular fusion proteins: a new superfamily. Proc. Natl. Acad. Sci. USA *94*, 3046–3051.

White, J., *et al*. (1999). Rab6 coordinates a novel Golgi to ER retrograde transport pathway in live cells. J. Cell Biol. *147*, 743–760.

Williams, B. C., Karr, T. L., Montgomery, J. M., and Goldberg, M. L. (1992). The *Drosophila l*(1) *zw10* gene product, required for accurate mitotic chromosome segregation, is redistributed at anaphase onset. J. Cell Biol. *118*, 759–773.

Williams, B. C., Li, Z.-X., Liu, S., Williams, E. V., Leung, G., Yen, T. J., and Goldberg, M. L. (2003). Zwilch, a new component of the ZW10/ROD complex required for kinetochore functions. Mol. Biol. Cell *14*, 1379–1391.

Wimmer, K., Zhu, X. X., Lamb, B. J., Kuick, R., Ambros, P. F., Kovar, H., Thoraval, D., Motyka, S., Alberts, J. R., and Hanash, S. M. (1999). Co-amplification of a novel gene, NAG, with the N-myc gene in neuroblastoma. Oncogene *18*, 233–238.

Xiao, J., Liu, C.-C., Chen, P.-L., and Lee, W.-H. (2001). RINT-1, a novel rad50-interacting protein, participates in radiation induced G2/M checkpoint control. J. Biol. Chem. *276*, 6105–6111.

Yang, J. S., Lee, S. Y., Spanò, S., Gad, H., Zhang, L., Nie, Z., Bonazzi, M., Corda, D., Luini, A., and Hsu, V. W. (2005). A role for BARS at the fission step of COPI vesicle formation from Golgi membrane. EMBO J. *24*, 4133–4143.

Yang, J. S., *et al*. (2008). A role for phosphatidic acid in COPI vesicle fission yields insights into Golgi maintenance. Nat. Cell Biol. *10*, 1146–1153.

Young, J., Stauber, T., del Nery, E., Vernos, I., Pepperkok, R., and Nilsson, T. (2005). Regulation of microtubule-dependent recycling at the *trans*-Golgi network by Rab6A and Rab6A′. Mol. Biol. Cell *16*, 162–177.

Zhang, T., Wong, S. H., Tang, B. L., Xu, Y., and Hong, W. (1999). Morphological and functional association of Sec22b/ERS-24 with the pre-Golgi intermediate compartment. Mol. Biol. Cell *10*, 435–453.

Zolov, S. N., and Lupashin, V. V. (2005). Cog3p depletion blocks vesicle mediated Golgi retrograde trafficking in HeLa cells. J. Cell Biol. *168*, 747–759.

Zuber, C., Fan, J. Y., Guhl, B., Parodi, A., Fessler, J. H., Parker, C., and Roth, J. (2001). Immunolocalization of UDP-glucose:glycoprotein glucosyltransferase indicates involvement of pre-Golgi intermediates in protein quality control. Proc. Natl. Acad. Sci .USA *98*, 10710–10715.